Conformations of Random Polyampholytes

Vesselin Yamakov [1,2,3], Andrey Milchev [1,2], Hans Jörg Limbach [1], Burkhard Dünweg [1] and Ralf Everaers [1]
[1] *Max–Planck–Institut für Polymerforschung, Postfach 3148, D–55021 Mainz, Germany*
[2] *Institute for Physical Chemistry, Bulgarian Academy of Sciences, G. Bonchev Street, Block 11, 1113 Sofia, Bulgaria*
[3] *Argonne National Laboratory, Materials Science Division, Build. 212, 9700 S. Cass Avenue, Argonne, IL–60439, USA*

We study the size R_g of random polyampholytes (i. e. polymers with randomly charged monomers) as a function of their length N. All results of our extensive Monte Carlo simulations can be rationalized in terms of the scaling theory we develop for the Kantor–Kardar necklace model, although this theory neglects the quenched disorder in the charge sequence along the chain. We find $\langle R_g \rangle \propto N^{1/2}$. The elongated globule model, the initial predictions of both Higgs and Joanny ($\propto N^{1/3}$) and Kantor and Kardar ($\propto N$), and previous numerical estimates are ruled out.

PACS Numbers: 61.41+e,82.70.Gg,64.75.+g

Polyampholytes (PAs) are heteropolymers comprising neutral, positively and negatively charged monomers. Such molecules are often water–soluble, offer numerous applications [1], and can be regarded as simple model systems for electrostatic interactions in proteins and other biopolymers. Depending on the method of synthesis, the charge sequence can either be alternating or random. The first case is well understood in terms of a theta collapse due to effectively short–ranged interactions [2,3]. In contrast, the statistical mechanics of random PAs [4–14] has turned out to be surprisingly complex. The purpose of this Letter is to settle a long–standing controversy on the shape of isolated random PAs in general and the effect of the quenched disorder in the charge sequence in particular.

The interest in this question was triggered by the discovery of Kantor and Kardar [7] that random PAs are sensitive to small disparities in the number of positively and negatively charged monomers per chain. In an ensemble of *statistically neutral* PAs of length N, the typical net charge is $|Q| \propto N^{1/2}$. Chains with a net charge up to this value behave as *globally neutral* ($Q \equiv 0$) PAs and form dilute globules of spherical shape as predicted by Higgs and Joanny [5]. In contrast, the more strongly charged members of the ensemble adopt strongly elongated conformations leading to a situation where ensemble averages for quantities such as the gyration radius for *statistically neutral* random PAs are dominated by the untypical, extended chains in the wings of the net charge distribution [7].

To explain this behavior Kantor and Kardar have proposed a model where, as a function of their net charge and in analogy to the Rayleigh instability of charged droplets, the PA globules split into a pearl–necklace–like sequence of smaller globules connected by thin strings [8,9]. While poly*electrolytes* (PEs) in poor solvent [15] are well described by the necklace concept [16,17], Kantor and Kardar have argued that in the PA case the charge inhomogeneities should drastically modify the necklace picture. Indeed, computer simulations of PAs reveal a rich variety of conformations [18] and it is unclear if the disorder is relevant for ensemble averages of quantities as the gyration radius $\langle R_g \rangle$. Ignoring all details of the charge sequence except the net charge, the necklace model predicts $\langle R_g \rangle \propto N^{1/2}$, while the evidence from Monte Carlo simulations [9] ($\langle R_g \rangle \propto N^{0.6}$) and exact enumerations [10] ($\langle R_g \rangle \propto N^{2/3}$) rather suggests a faster growth. Nevertheless, the effect seems to be weaker than predicted [6] by Kantor's and Kardar's original renormalization group argument ($\langle R_g \rangle \propto N$).

In the following we present a complete scaling theory for the Kantor–Kardar necklace model as well as large scale computer simulations of various ensembles of quenched random PAs: Fixed (zero or nonzero) net charge, and randomly charged chains with a typical net charge of order $N^{1/2}$. With respect to the length of our chains $N \leq 4096$ as well as the number of independent charge sequences (between 512 and 1024) we by far exceed previous simulation studies [9,18,19]. The good statistics for large chains turns out to be crucial, since our results suggest that deviations from the predictions of the necklace model for *ensemble averages* are merely finite size effects.

We consider isolated, flexible chains of N monomers of diameter b in a good solvent with no added salt. This corresponds to the limit of *infinite* dilution, where the chains do not form complexes [13] and where counterions, which may be necessary to balance the net charge of the considered PA ensemble, can be considered as infinitely far away. For a particular chain, a fraction $f = f_+ + f_-$ of the monomers at quenched random positions carries charges $\pm e$, resulting in a net charge per monomer of $e\delta f = e(f_+ - f_-)$. The strength of the unscreened electrostatic interactions is characterized by the Bjerrum length, $l_B = e^2/(\epsilon k_B T)$.

Globally *neutral* chains ($\delta f \equiv 0$) assume a globular conformation if they are sufficiently long [5], while for shorter chains a smooth crossover to self–avoiding walks (SAWs) occurs. Within the framework of mean field theory, the attraction energy is estimated via the Debye–Hückel polarization energy density [4] $f_{DH} \propto \kappa^3 k_B T$, where the inverse squared screening length $\kappa^2 = l_B f c$ is proportional to the monomer concentration c. Thus the attraction will be important on length scales larger than the so called blob diameter $\xi_a = \kappa^{-1}$. On length scales below ξ_a the conformation is described as an un-

perturbed SAW, so that $\xi_a = b g_a^\nu$, where g_a is the number of monomers in the blob, and $\nu \approx 0.59$. Since $c = g_a/\xi_a^3$, the blob size is given as $g_a = (b/(l_B f))^{1/(1-\nu)}$. The PA chain is then envisioned as a spherical droplet of blobs; this minimizes the surface energy which is estimated as $(N/g_a)^{2/3} k_B T$ (each surface blob contributes $k_B T$). The gyration radius hence scales as

$$\frac{R_g^2(\delta f \equiv 0, f, l_B/b, N)}{R_{SAW}^2} \propto \begin{cases} 1 & N/g_a \ll 1, \\ \left(\frac{N}{g_a}\right)^{2(1/3-\nu)} & N/g_a \gg 1. \end{cases} \quad (1)$$

In analogy to Khokhlov's description of PEs in poor solvent [15], a first understanding of the effect of a nonzero net charge density δf can be gained from an elongated globule model [1,11,12]. A globule becomes extended as soon as the Coulomb energy $k_B T (\delta f N)^2 l_B / \left((N/g_a)^{1/3} \xi_a\right)$ exceeds the surface energy $k_B T (N/g_a)^{2/3}$, i. e. for $N > g_R = f/\delta f^2$, the number of monomers in a "Rayleigh blob", whose size is given by $\xi_R = \xi_a (g_R/g_a)^{1/3}$. The globule is stable for $g_a < N < g_R$, while for $N > g_R$ the elongated globule model predicts an object of diameter ξ_R and length $(N/g_R)\xi_R$, whose relative extension is thus given by

$$\frac{R_g^2(\delta f, f, l_B/b, N)}{R_g^2(\delta f \equiv 0, f, l_B/b, N)} \propto \begin{cases} 1 & N/g_R \ll 1, \\ \left(\frac{N}{g_R}\right)^{4/3} & N/g_R \gg 1. \end{cases} \quad (2)$$

However, Kantor and Kardar [8,9] argued that the electrostatic repulsion should rather result in necklace–like conformations, where spherical regions with net charges below the instability threshold alternate with thin strings. Based on this concept, Dobrynin et al. [16] developed a scaling theory for PEs in poor solvent, which has been recently shown in computer simulations to describe the data much better than the earlier Khokhlov picture [17]. Applied to PAs, one expects the pearl and string diameters to be given by ξ_R and ξ_a respectively. The length $l = \xi_R (\xi_R/\xi_a)^{1/2} \gg \xi_R$ of the strings is then again determined by the equilibrium between the additional surface energy of the strings, $k_B T l/\xi_a$, and the electrostatic repulsion between the pearls, $k_B T (\delta f g_R)^2 l_B/l$. Note that even though the strings make up for most of the length of the necklace, they contain only a negligible fraction of the PA volume, with $R_g(\delta f, N) = (N/g_R) l$. Hence the necklace model predicts a different scaling for the chain dimensions,

$$\frac{R_g^2(\delta f, f, l_B/b, N)}{R_g^2(\delta f \equiv 0, f, l_B/b, N)} \propto \frac{\xi_R}{\xi_a} \left(\frac{N}{g_R}\right)^{4/3}, \quad N/g_R \gg 1, \quad (3)$$

than the elongated globule model, Eq. (2). It should be noted that in the necklace case no universal scaling function of just one scaling argument N/g_R occurs, i. e. a complete data collapse is only possible for *either* the globular regime *or* the necklace regime, the reason being that the regimes are separated by a first–order phase transition [16,17]. Conversely, the elongated globule model predicts just a smooth crossover, such that only a single scaling function occurs.

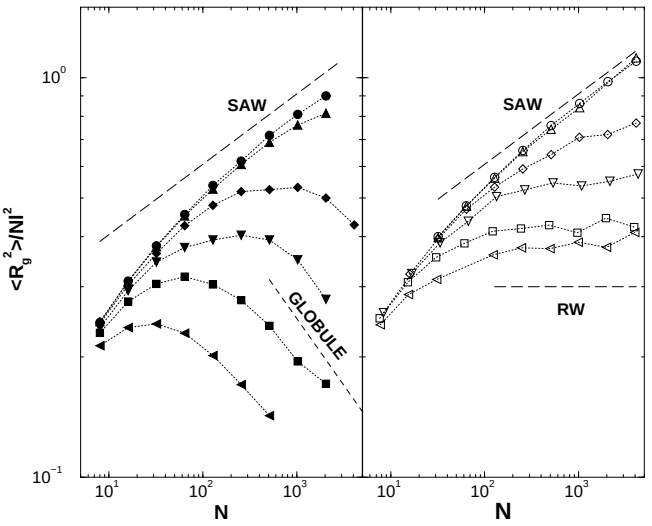

FIG. 1. Radius of gyration as a function of chain length N for (a) globally (full symbols) and (b) statistically (open symbols) neutral random PAs with $l_B/b = 1/64\,(\circ),\ 1/16\,(\triangle),\ 1/4\,(\diamond),\ 1/2\,(\triangledown),\ 1\,(\square),\ 2\,(\triangleleft)$. The data are normalized to the size of random walks, while the straight lines indicate the slopes expected for self–avoiding walk ($R_g \propto N^\nu$, $\nu = 0.588$), random walk ($R_g \propto N^{1/2}$) and globular($R_g \propto N^{1/3}$) conformations.

Finally we consider the ensemble treated by Kantor and Kardar, randomly charged PAs with a Gaussian net charge distribution of zero mean and width $\langle \delta f^2 \rangle = f/N$. The calculation of averages such as $\langle R_g \rangle$ is somewhat subtle. For $N \ll g_a$ one will of course observe SAW behavior, while for $N \gg g_a$ the ensemble comprises contributions from both the globular and the necklace phase. Indeed, each charge realization implies a certain value of $g_R = f/\delta f^2$, the typical value being $g_R = N$. Hence there will always be a finite (N–independent) fraction of chains whose g_R is small enough that they are in the extended necklace phase. This fraction will asymptotically dominate the average value of R_g. Thus the average stretching relative to the globule is found by just using Eq. (3), where g_R is replaced by N. Since then $\xi_R/\xi_a = (g_R/g_a)^{1/3} = (N/g_a)^{1/3}$, we find

$$\frac{R_g^2(\langle \delta f \rangle = 0, f, l_B/b, N)}{R_g^2(\delta f \equiv 0, f, l_B/b, N)} \propto \begin{cases} 1 & N/g_a \ll 1, \\ \left(\frac{N}{g_a}\right)^{1/3} & N/g_a \gg 1. \end{cases} \quad (4)$$

One thus finds $\langle R_g \rangle \propto N^{1/2}$ for the random PA necklace [8,9], which is formally a random walk (RW) exponent, while the underlying structure is completely different. Note that within the elongated globule model (i. e. disregarding the possibility of a Rayleigh instability) the net charge fluctuations are predicted to be irrelevant as originally assumed by Higgs and Joanny [5].

In our Monte Carlo simulations we studied a bead–spring model with short–range potentials to model connectivity and excluded volume. All monomers are charged ($f = 1$) and

interact via an unscreened Coulomb potential. This yields the largest amount of charge fluctuations with the smallest number of monomers, while we are not interested in details of the chain structure below the distance between neighboring charges. We varied the blob size g_a by studying different values of $l_B/b = 1/64 \ldots 4$. Note that in order to reach the $\mathcal{O}(10^3)$ blobs necessary for the formation of well–defined globules and necklaces, we had to push the strength of the electrostatic interaction to or even slightly beyond the validity limit ($l_B/b = \mathcal{O}(1)$) of the blob picture.

Further factors which facilitated the feasibility of the investigation were the use of a large parallel computer, exploiting the inherent parallelism resulting from the disorder realizations, plus the application of a very efficient hybrid algorithm which combines local moves with the pivot technique [20], while starting off from a configuration that was generated via the enhanced configurational biased Monte Carlo method [21] with already equilibrated bond lengths. At each state point we studied 512 or 1024 different realizations of the disorder, each of which was observed for a fixed run time. For the shorter chains and smaller charges, this run time was long enough to yield a few hundred statistically independent configurations per realization (as estimated via the autocorrelation function of the end–to–end vector). On the other hand, the long globally neutral chains at strong charging were very difficult to equilibrate in their dense globular state. Reasonable statistics (with at least a few ten independent configurations) is available up to $l_B/b = 1$, while for $l_B/b = 2$ only the data up to $N = 512$ are reliable. For $l_B/b = 4$ the globular state was practically inaccessible, and only necklaces could be studied. For further details we refer the reader to Ref. [22], where the analogous model was simulated with the same methods to study PE adsorption. All in all, we needed roughly 5×10^4 hours single–processor CPU time for the calculation.

Figure 1 shows the chain length dependence of the gyration radii of globally (full symbols) and statistically (open symbols) neutral random PAs. The data show unequivocally that sufficiently long random PAs with a global neutrality constraint adopt globular conformations ($R_g \propto N^{1/3}$), while unconstrained random PAs are on the average significantly more extended, with $R_g \propto N^{1/2}$. Clearly, a growth of R_g with N which is even faster than that of the SAW, as was suggested by Refs. [9,10], can be ruled out.

The corresponding scaling plot (Fig. 2) supports the Higgs and Joanny [5] picture of the behavior of globally neutral chains as well as our formulation of the necklace model for PAs carrying a net charge. For the SAW data we took those with the weakest charge $l_B/b = 1/64$, which is very close to the true SAW behavior for our chain lengths. One also sees that the crossover from the SAW into the globule is subject to considerable corrections to scaling, which are probably mainly due to the rather small g_a values of our simulation.

In order to better characterize the Rayleigh instability we also investigated ensembles of random PAs with a fixed nonzero net charge. Figure 3 demonstrates that the elongated globule model describes the onset of the deformation up to

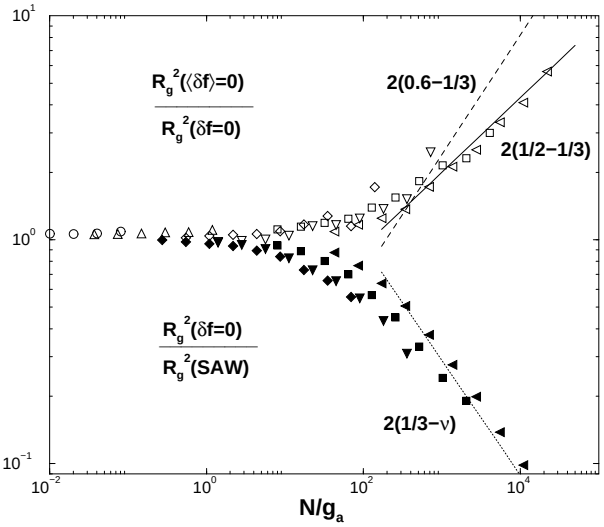

FIG. 2. Scaling plot of the data presented in Fig. 1. The full symbols show the shrinking of globally neutral PAs relative to uncharged SAWs, while the open symbols represent the swelling of *statistically* neutral relative to *globally* neutral PAs. The data are plotted as a function of the reduced chain length N/g_a and support Eq. (1) and, in particular, the prediction Eq. (4) of the necklace model. The dashed line corresponds to the earlier numerical estimate $R_g \propto N^{0.6}$ [9], which is clearly not supported by the data.

elongations by about a factor of two. The Rayleigh instability occurs around $N/g_R \approx 2$, while for $N/g_R > 3$ the data are in excellent agreement with the prediction Eq. (3) of the necklace model.

Quite interestingly, the exponent $1/2$ even seems to characterize the ensemble averages for the mean square internal distances $\langle r_{ij}^2 \rangle \equiv \langle (\vec{r}_i - \vec{r}_j)^2 \rangle$ in statistically neutral PAs (see the inset in Fig 4). That random PAs are, however, far from being random-walk like fractal objects is demonstrated by the structure factor $S(k)$ ($\times$ in Fig. 4) which clearly deviates from the Debye function. For comparison, we have also calculated $S(k)$ in the Gaussian approximation $\langle \exp[i\vec{k} \cdot \vec{r}_{ij}] \rangle = \exp[-k^2 \langle r_{ij}^2 \rangle / 2]$ showing that the distribution function $p(r_{ij})$ cannot be specified by its second moment alone.

In summary, our results have demonstrated a remarkable success of the simple necklace model for random polyampholytes. In particular, the scaling of the *average* extension of the chains is not affected by the quenched disorder of the charge positions along the chains. Nevertheless, a more detailed description of the relation between the charge sequence on individual chains and their typical conformations remains a challenge.

This work was supported by collaboration grant number I/72 164 from the Volkswagen foundation. We thank the Rechenzentrum Garching for generous allocation of Cray T3E CPU time.

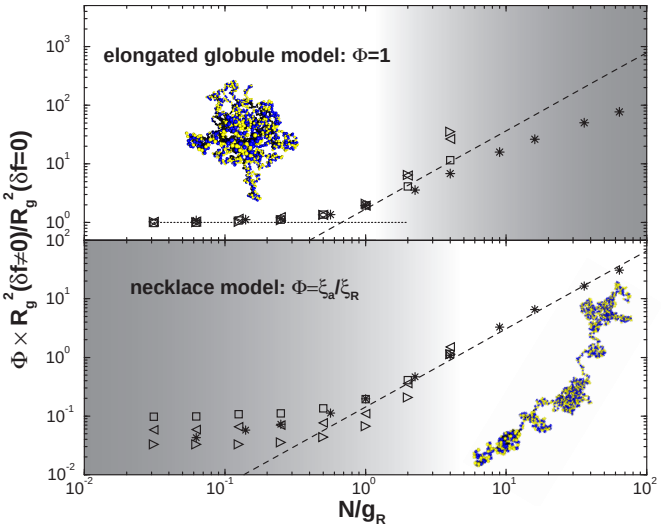

FIG. 3. Swelling of random PAs due to a nonzero net charge density $\delta f > 0$. We show three data sets $l_B/b = 1\ (\square),\ 2\ (\triangleleft),\ 4\ (\triangleright)$ for systems with fixed asymmetry $\delta f = 1/32$, and varying chain lengths $32 \le N \le 4096$ and one data set with $l_B/b = 1\ (\star)$, fixed chain length $N = 1024$ and charge asymmetries $1/128 \le \delta f \le 1/2$. The shaded areas indicate the parameter regions where the scaling forms Eq. (2) and (3) break down, corresponding to the elongated globule and the necklace model, respectively. The dashed line represents the function $(N/g_R)^{4/3}$ predicted by both models for $N/g_R \gg 1$. The insets show typical conformations for chains with $N = 1024$ and $l_B/b = 4$ with $\delta f = 0$ and $N/g_R = 4$, respectively.

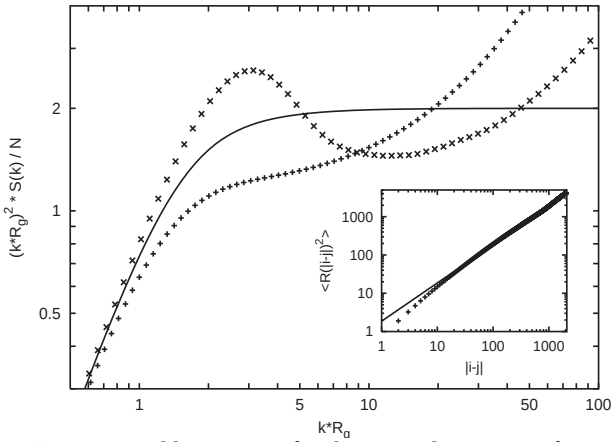

FIG. 4. Ensemble averages for the internal structure of statistically neutral random PAs with $N = 2048$ and $l_B/b = 1$. The $+$ symbols in the inset show the mean square distance $\langle r_{ij}^2 \rangle$ of two monomers as a function of their distance $|i-j|$ along the chain in comparison to a $|i-j|^{2\times 1/2}$ power law. The figure shows the structure factor $S(k)$ $(\times)$ in the Kratky representation as a function of kR_g in comparison to the Debye function (solid line) for random-walk like fractal objects and the result one obtains in the Gaussian approximation from the data in the inset $(+)$.

[1] F. Candau and J.-F. Joanny, in *Polymeric Materials Encyclopedia*, edited by J. C. Salamone (CRC Press, Boca Raton, 1996).
[2] J. M. Victor and J. B. Imbert, Europhys. Lett. **24**, 189 (1993).
[3] J. Wittmer, A. Johner, and J.-F. Joanny, Europhys. Lett. **24**, 263 (1993).
[4] S. F. Edwards, P. R. King, and P. Pincus, Ferroelectrics **30**, 3 (1980).
[5] P. Higgs and J.-F. Joanny, J. Chem. Phys. **94**, 1543 (1991).
[6] Y. Kantor and M. Kardar, Europhys. Lett. **14**, 421 (1991).
[7] Y. Kantor, H. Li, and M. Kardar, Phys. Rev. Lett. **69**, 61 (1992); Phys. Rev. E **49**, 1383 (1994).
[8] Y. Kantor and M. Kardar, Europhys. Lett. **27**, 643 (1994).
[9] Y. Kantor and M. Kardar, Phys. Rev. E **51**, 1299 (1995).
[10] Y. Kantor and M. Kardar, Phys. Rev. E **52**, 835 (1995).
[11] A. Gutin and E. Shakhnovich, Phys. Rev. E **50**, R3322 (1994).
[12] A. V. Dobrynin and M. Rubinstein, J. de Physique II **5**, 677 (1995).
[13] R. Everaers, A. Johner, and J.-F. Joanny, Europhys. Lett. **37**, 275 (1997); Macromolecules **30**, 8478 (1997).
[14] Y. Kantor *et al.*, Phys. Rev. E **53**, 846 (1996); Phys. Rev. E **55**, 261 (1997); Phys. Rev. E **57**, 5719 (1998).
[15] A. Khokhlov, J. Phys. A **13**, 979 (1980).
[16] A. V. Dobrynin, M. Rubinstein, and S. P. Obukhov, Macromolecules **29**, 2974 (1996).
[17] A. Lyulin, B. Dünweg, O. Borisov, and A. A. Darinskii, Macromolecules **32**, 3264 (1999).
[18] N. Lee and S. Obukhov, Europ. Phys. J. B **1**, 371 (1998).
[19] M. Tanaka *et al.*, Phys. Rev. E **56**, 5798 (1997); J. Chem. Phys. **110**, 8176 (1999); Langmuir **15**, 4052 (1999).
[20] N. Madras and A. D. Sokal, J. Stat. Phys. **50**, 109 (1988).
[21] D. Frenkel and B. Smit, *Understanding Molecular Simulation: From Algorithms to Application* (Academic Press, NY, 1996).
[22] V. Yamakov, A. Milchev, O. Borisov, and B. Dünweg, J. Phys. Condens. Matter **11**, 9907 (1999).